Indian Journal of Biochemistry & Biophysics
Vol. 63, November 2026, pp. 1327-1346
DOI: 10.56042/ijbb.v63i11.31002

Synthesis of quinoline carboxamide analogues and comprehensive evaluation of their biological activities using bioactivity aware hybrid machine learning framework

Shunmugaraj Patchaikani*, and Thankappan Florence Inpam Abbs Fen Reji

Department of Chemistry, Nesamony Memorial Christian College, Marthandam-629 165, Tamil Nadu, India

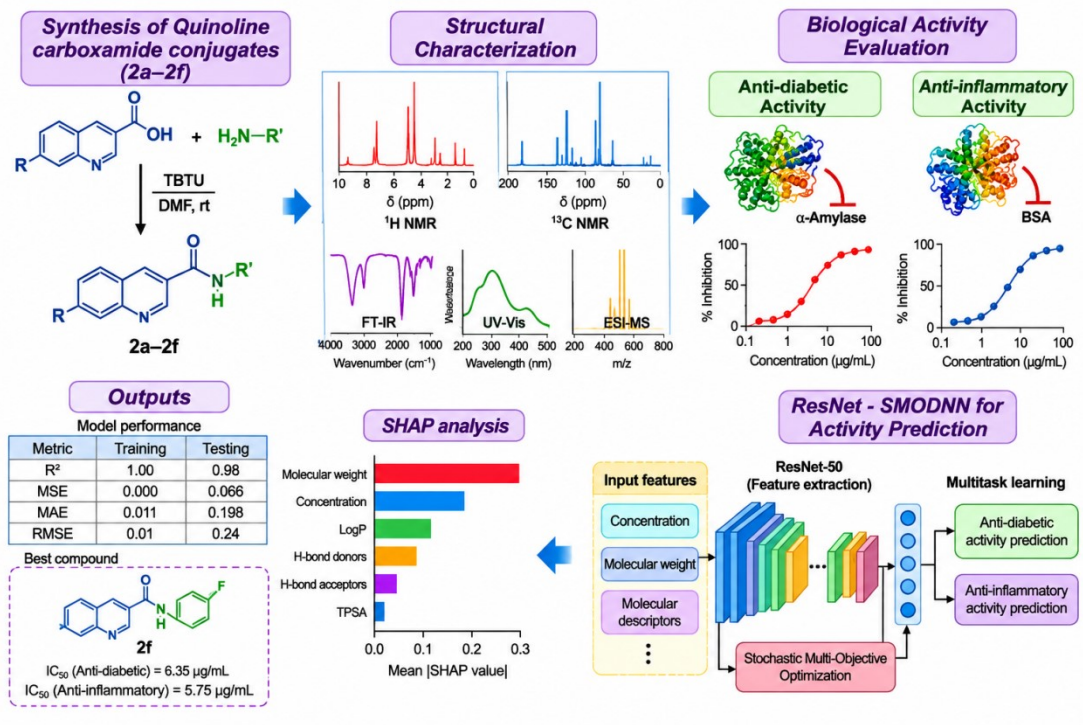
Received 20 April 2026; *revised 28 September 2026*

A series of six quinoline–carboxamide conjugates (2a–2f) prepared and screened at various concentrations for their anti-diabetic and anti-inflammatory effects in this research. The synthesis involved coupling quinoline carboxylic acid derivatives with several amines by means of O-(Benzotriazol-1-yl)-N, N, N', N'-tetramethyluronium tetrafluoroborate (TBTU) mediated amidation. Structural characterization is confirmed by 1H and 13C- NMR, FT-IR, UV-Vis, and ESI-MS. The biological activities are assessed using BSA denaturation and α-amylase inhibition assays. A Residual Network-50-based Stochastic Multi-Objective Optimized Deep Neural Network (ResNet -SMODNN) with multitask learning developed to predict the anti-diabetic and anti-inflammatory activities of quinoline–carboxamide conjugates (2a–2f). The model developed with the concentration dependent parameters and molecular descriptors such as molecular weight to explain the relationship among the compound properties and biological activity. It demonstrated excellent predictive performance with a coefficient of determination, MSE, MAE and RMSE of 1.00, 0.000, 0.011, 0.01 for training and 0.86, 0.056, 0.189 and 0.24 for testing, respectively. Among the synthesized derivatives, compound 2f had the best observed activity with experimentally determined IC_{50} values of 6.35 µg/mL and 5.75 µg/mL for anti-diabetic and anti-inflammatory activities, respectively. According to SHAP analysis, the contribution of molecular weight the largest for the input features considered in the explored dataset. The hybrid machine learning approach gives a preliminary computational method for the bioactivity prioritization of quinoline–carboxamide derivatives and help in future experimental studies.

Keywords: Anti-diabetic activity, Anti-inflammatory activity, Concentration, Machine Learning, Quinoline carboxamide, SHapley additive exPlanations analysis

Hybrid pharmacophores have been found to be an effective method of developing drugs with high therapeutic value. The combinations of quinoline and carboxamide are the most appropriate combinations that enhance the therapeutic potential and selectivity of drugs. These compounds are of great importance because they have the capability of solving several biological issues, such as metabolism and other disorders related to inflammatory processes[1-2]. Quinoline is a nitrogen-based heterocyclic compound, and it is famous due to its large variety of pharmacology, such as antimicrobial, anticancer, anti-inflammatory, and anti-diabetic effects[3]. Its capacity to react with enzymes, receptors and nucleic acids, combined with high modifiability of the structure, is beneficial in the optimization of physicochemical properties, pharmacokinetic properties to achieve drug-likeness[4-5]. The carboxamide group is also equally versatile in drug design, which aids in the attainment of a higher level of molecular recognition and interaction based on hydrogen bonding and dipolar effects, thus improving specificity and stability[8,9]. The carboxamide-functionalized molecules have in fact, shown remarkable therapeutic effects like the anti-inflammatory, anti-diabetic, anti-cancer, anti-viral and anti-microbial effects coupled with excellent membrane permeability and chemical stability[6]. The quinoline and carboxamide groups interact, thus forming hybrids with enhanced bioactivity in addition to bioavailability[7]. These hybrids act based on modulating key metabolic pathways such as Peroxisome Proliferator-Activated Receptors (PPARs), Dipeptidyl Peptidase-4 (DPP-4), and β-glucosidase with a better glycemia level, and also suppressing the action of agents of inflammation like Tumour Necrosis Factor-alpha (TNF-α), Interleukin-6 (IL-6) and Cycloxygenase-2 (COX-2)[8-9]. Thus, it has been demonstrated that quinoline carboxamide hybrids serve as a good substrate in the construction of next-generation therapeutic agents that be used as anti-diabetic agents and as anti-inflammatory agents[10].

*Correspondence:
E-mail: pshunmugaraj25@gmail.com



Graphical abstract

Quinoline–carboxamide conjugates possess significant pharmacological potential, yet there is a notable lack of integration between computational approaches and experimental evaluations in existing research. Most studies emphasize conventional synthesis and standard biological assays, leading to an insufficient understanding of the non-linear relationships with molecular structure and biological activity. Traditional methods are time-consuming and costly, which restricts scalability in drug discovery. Prior computational analyses have focused on anti-diabetic or anti-inflammatory effects individually, neglecting multitask learning frameworks that could predict both simultaneously. There is also a deficit in bioactivity-aware predictive models that include relevant experimental features such as concentration and molecular weight. Furthermore, the use of interpretable Machine Learning (ML) methods and deep learning architectures, such as ResNet-50 with graph neural networks, remains largely unexplored. These issues underscore the necessity for a hybrid framework that integrates chemical synthesis, biological validation, and advanced ML to expedite the development of new quinoline-based therapeutics.

Şahin *et al.*[11] investigated a synergistic approach involving the use of a Genetic Algorithm (GA) and 4-Dimensional Quantitative Structure-Activity Relationship (4D-QSAR) to predict the bioactivity of quinazoline analogues. Therefore, the results show that the hybrid Gradient Boosting Machine-based Random Forest (GBM + RF) model had the best predictive performance with a correlation coefficient, R^2 of 0.9978, which shows that the model is almost perfect in predicting the actual value.

Sun *et al.*[12] proposed an Artificial Neural Network (ANN) approach that employed Simplified Molecular Input Line Entry System (SMILES) strings and quantum chemical descriptors to determine the site selectivity of C-H functionalization in quinoline derivatives. The accuracy in the external validation set is 86.5%, but restricted by the use of existing descriptors that necessitate large amounts of data.

Naglah *et al.*[13] synthesized pyrazole-based Schiff bases and evaluated their antioxidant, anti-diabetic, anti-Alzheimer's, anti-inflammatory, and anticancer activities. Some of the selected compounds were found to be very cytotoxic to lung (A549) and Cancer Coli-2 (Caco-2) cells and had good enzymatic and in silico Absorption, Distribution, Metabolism, Excretion, and Toxicity (ADMT) profiles, suggesting their utility as multi-target therapeutic agents.

da Silva *et al.*[14] synthesized quinoline-thiazolidinedione hybrids and showed their anti-inflammatory action by cytokine inhibition.

Compounds like Z)-5-(4-bromobenzylidene)-3-(quinolin-2-ylmethyl)thiazolidine-2,4-dione (LPSF/ZKD-2) and (Z)-5-(4-(dimethylamino) benzy lidene)-3-(quinolin-2-ylmethyl)thiazolidine-2,4-dione (LPSF/ZKD7) were shown to have a significant dose-dependent reduction of Interferon-7 (IFN- 7) and Tumor Necrosis Factor-alpha-2 (TNF- 2), whereas LPSF/ZKD4 had a strong inhibition of Interleukin-6 (IL-6) expression and showed a high Peroxisome Proliferators Activated Receptor (PPAR- 7) agonist. High binding affinity to PPAR7 and cyclooxygenase-2 (COX-2) was verified by docking analysis, and the hybrids of quinoline and thiazolidinedione were found to be promising and useful anti-inflammatory drugs.

Alharbi *et al.*[15] prepared quinoline-naphthalene hydrazineylidene-propenamide derivatives as anti-diabetics. Enzyme inhibition against α-glucosidase, α-amylase and aldose reductase was evaluated in the research with the backing of molecular docking and molecular dynamics simulations, whereby compound 7g exhibited better inhibitory behavior and binding stability as compared to the standard drugs.

Arabiyat *et al.*[16] evaluated quinoline derivatives and fluoroquinolones with *in vitro* anti-inflammatory properties on Lipo Poly Saccharides (LPS) stimulated RAW264.7 macrophages and cytotoxicity screen on various cancer cell lines, with results showing potent anti-inflammatory properties and specific antiproliferative effects, especially against Michigan Cancer Foundation-7 (MCF7) and Henrietta Lacks (HELA) cells.

Aarjane *et al.*[17] introduced the oxadiazole, acylhydrazone, and pyrazolone moieties and explored ML models with the prediction of antimicrobial activity, disclosing promising candidates that showed strong predicted efficacy together with favourable molecular docking interactions, as well as acceptable profiles regarding ADMET.

Marciniec *et al.*[18] developed 22 hybrids of 8-quinolinesulfonamide and 1,4-disubstituted triazole that had antiproliferative properties through the use of molecular modelling, ML, molecular docking, and dynamics. The synthesis was done using copper-catalyzed azide-alkyne cycloaddition. The research indicates that future developments in cancer treatment seen through the improvement of the quinolinyl structure that would improve cytotoxicity.

The rising incidence of inflammatory and metabolic disorders and the limitations of current anti-inflammatory and anti-diabetic medications underscore the need for safer, more effective therapies. Although quinoline-based compounds show promising pharmacological properties, traditional methods for developing new derivatives are often slow, expensive, and resource-consuming. The intricate dependency between molecular structure and biological activity hampers conventional screening efficacy. There is an absence of comprehensive frameworks integrating rational synthesis, experimental validation, and advanced ML techniques to predict and optimize the bioactivity of quinoline–carboxamide conjugates. A hybrid approach that fuses experimental methods with data-driven modeling is essential to improve drug discovery efficiency and reduce development time and costs. The research objective of the proposed research is as follows:

- To synthesis six quinoline–carboxamide conjugates (2a, 2b, 2c, 2d, 2e and 2f) and evaluation of their anti-diabetic and anti-inflammatory activities at different concentration levels.
- The prepared compound is Structurally characterized.
- To develop a bioactivity-aware ML framework for predicting anti-diabetic and anti-inflammatory activities of synthesized quinoline–carboxamide derivatives using molecular and experimental descriptors.
- To build a ML model to predict the anti-diabetic and anti-inflammatory activities of synthetic quinoline–carboxamide derivatives using molecular descriptors and experimental descriptors that are bioactivity aware.
- To assess the predictive performance of the proposed method using statistical metrics such as the coefficient of determination (R2), Mean Squared Error (MSE), Mean Absolute Error (MAE), Along with Root Mean Squared Error (RMSE)
- To interpret the contribution and significance of input features influencing bioactivity prediction using SHapley Additive exPlanations (SHAP) analysis.
- To assess the predictive power of the proposed framework with compound-level validation and explainability of the contribution of the input features by applying explainable ML methods.

The research paper is organized into four sections: Section 1 conveys the introduction part, the literature review, and research objectives, Section 2 addresses the suggested methodology, Section 3 describes the

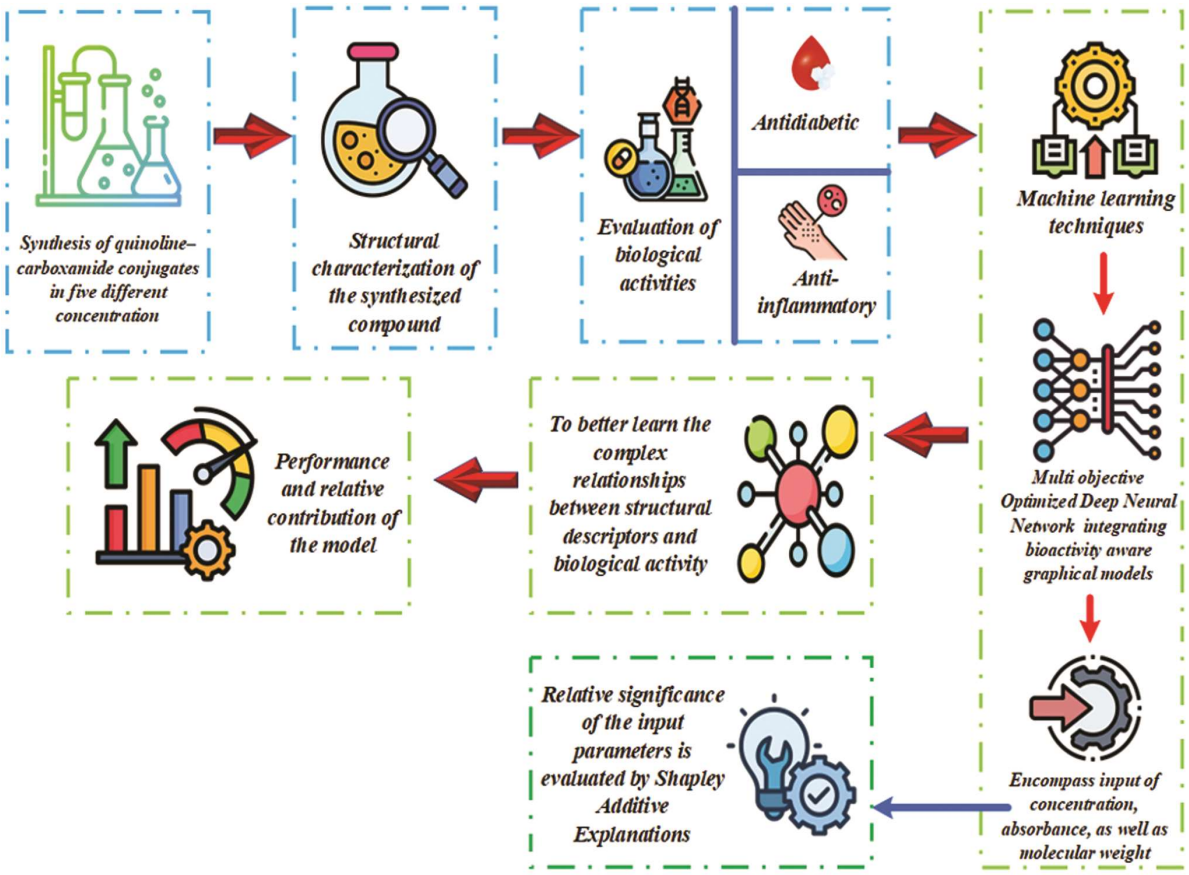


Fig. 1 — Proposed architecture of quinoline–carboxamide hybrid modeling framework

research findings, and Section 4 is focused on the research's conclusion and future prospects.

Proposed architecture of the proposed quinoline–carboxamide hybrid modeling framework

The proposed quinoline-carboxamide hybrid modeling framework is developed based on the integration of chemical synthesis, structural characterization, *in vitro* biological evaluation, and advanced ML modeling for predicting anti-diabetic and anti-inflammatory bioactivities. The framework is developed using experimental data obtained from six synthesized quinoline–carboxamide derivatives (2a–2f), which are evaluated at multiple concentration levels for biological activity assessment.

Figure 1 depicts the overall workflow of the proposed hybrid experimental and ML -based approach for analysis of the anti-diabetic and anti-inflammatory potential of quinoline carboxamide conjugates. The first step includes the synthesis of six quinoline–carboxamide derivatives (2a–2f) and further evaluation in biological tests at various concentrations**.** Subsequently, the detailed structural characterization of the conjugates is carried out by employing standard analytical techniques to establish the integrity of the molecules. The synthesized conjugates are then subjected to experimental evaluation of drug activity to assess the anti-diabetic and anti-inflammatory potential by employing *in vitro*-based experimental approaches. The experimentally obtained data is employed as input data for the proposed ML approach. The optimized deep neural network coupled with the graphical model is used to build non-linear correlations involving the structural parameters. The model integrates essential experimental input parameters, which include concentration, absorbance, and molecular weight. Multitask learning is employed in the model to enable generalization. The performance of the proposed model is assessed based on several statistical measures. Additionally, the contribution of the proposed model is assessed by quantifying the parameter input significance utilizing the SHAP technique. Nevertheless, the proposed model is efficient in chemical synthesis, biological experimentations, and the utilization of ML techniques in bioactivity prediction with quinoline compounds. The proposed model is efficient due to the effective integration of

chemical synthesis, biological experimentations, and ML techniques. The utilization of multitask learning ascertains the robust performance of the model. Additionally, the model is efficient in performing the prediction of the bioactivity of quinoline compounds.

Methods and experimental section

This section details the synthetic procedures for quinoline carboxamide derivatives and the *in vitro* biological analysis of their anti-inflammatory and anti-diabetic activities. It also describes the computational framework employing a ResNet-50-based SMODNN for predicting these bioactivities using spectroscopic data, molecular descriptors, and assay results. All experiments are conducted with appropriate controls, and analytical techniques ensured reaction monitoring and data accuracy.

Synthesis of quinoline carboxamide derivatives

Quinoline carboxylic acid (1.0 equiv) was dissolved in acetonitrile, followed by the addition of TBTU (1.1 equiv) and Tri Ethyl Amine (TEA) (2.0 equiv). The reaction mixture was stirred at room temperature for 30 min to activate the carboxylic acid. Subsequently, the amine (1.1 equiv) was added, and the reaction mixture was stirred at room temperature for an additional 6 h to facilitate amide formation. Thin-layer chromatography (TLC) is used to monitor the progress of the reaction. The solvent has been removed under reduced pressure and the residue is extracted with ethyl acetate to give the corresponding quinoline–carboxamide derivatives 2a–2f. The chemical synthesis of the quinoline compound and its derivatives is shown in (Fig. 2).

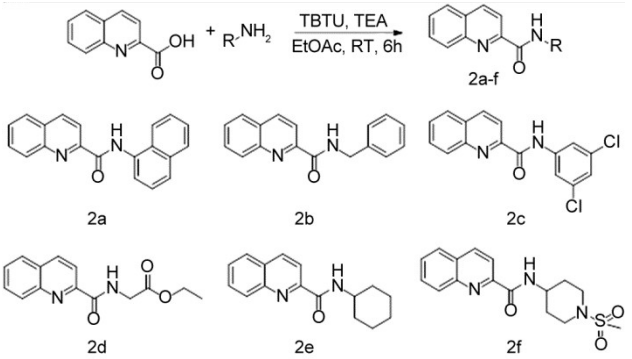


Fig. 2 — Chemical synthesis of the quinoline compound and its derivatives

The structural and physicochemical properties of the synthesized quinoline–carboxamide derivatives (2a–2f) along with their molecular characteristics, hydrogen-bonding property, polarity and lipophilicity trends are summarized in (Table 1). The yields and melting points of the synthesized compounds (2a–2f) are presented in (Table 2), which has been used for further characterization and purity test of the synthesized compounds.

Anti-inflammatory activity using the Bovine Serum Albumin (BSA) denaturation technique

BSA denaturation assay performed as *in vitro* screening assay to determine the prevention of protein

Table 2 — Reaction Yields and Melting Point Values of Synthesized Quinoline–Carboxamide Derivatives (2a–2f)

Compounds	Reaction Yields (%)	Melting points (°C)
2a	80-82	143-144
2b	81-83	120-121
2c	84-85	133-134
2d	83-85	103-104
2e	82-84	98-99
2f	85-86	138-139

Table 1 — Structural and Physicochemical Properties of Compounds 2a–2f

Compounds	R Group Description	Molecular Nature	H-Bond Donor (HBD)	H-Bond Acceptor (HBA)	Relative Polarity	Expected Lipophilicity (LogP trend)	Structural Remark
2a	Aniline (phenyl)	Aromatic amide	1	2	Low–Moderate	High	Increased aromatic π-system
2b	Benzyl	Aromatic–aliphatic	1	2	Moderate	Moderate–High	Flexible benzylic spacer
2c	3,4-Dichlorophenyl	Halogenated aromatic	1	2	Low	Very High	Electron-withdrawing Cl groups increase hydrophobicity
2d	Ethyl carbamate	Ester-containing	1	3	Moderate–High	Moderate	Additional carbonyl increases polarity
2e	Cyclohexyl	Alicyclic	1	2	Low	High	Non-aromatic hydrophobic ring
2f	Piperazine sulfonyl	Heterocyclic sulfonamide	1	4	High	Low–Moderate	Highly polar due to sulfonyl group

denaturation under induced stress conditions. The activity seen in this assay is not a direct measure of inhibition of specific inflammatory enzymes and molecular targets, and is interpreted as inhibition of protein denaturation and a potential anti-inflammatory activity.

The newly synthesized compound, as well as the reference compound diclofenac sodium, are tested for anti-inflammatory activity by an inhibition of albumin denaturation test with slight changes. Solutions of the reference compound as well as the newly synthesized compound are prepared by dissolving the compounds in the minimum required Dimethyl formamide (DMF) and making it up with 0.2 M phosphate buffer solution, pH 7.4. The final concentration of DMF with test solution should be below 2.5%. Similarly, the test solution, containing 2.5 mL of a solution containing a certain amount of drug, 1 mL of 1 mM BSA solution, prepared using a phosphate buffer of pH 7.4, incubated at 37°C using an incubator. The denaturation process of BSA[19] accelerated by incubating the solution mixture with 1 mL of BSA solution in a boiling water bath at 70°C for 10 min. Then, after stopping the incubation, solutions are allowed to cool. The turbidity of solution measured using a spectrophotometer set at 660 nm. The percentage inhibition of denaturation calculated from the control solution, in which no drug added using the following formula.

$$\%\ of\ inhibition = 100 * \left(\frac{A_c - A_t}{A_c} \right) \quad \ldots (1)$$

whereas, A_t defines the test absorbance and A_c states the control absorbance.

Anti-diabetic activity using the α-amylase inhibition technique

Anti-diabetic activity of sample assessed by the α-amylase inhibition method [20]. In this method, Amylase (0.2%) is mixed and incubated in the presence of absence of the sample and standard, along with 1.5 mL. Incubation is done for 10 min at 25°C temperature. Similarly, the experiment is conducted by using 0.2 M phosphate buffer having a pH of 6.9. After incubation, 1% of starch solution (0.5mL) is mixed and incubated for 30 min at a temperature of 25°C. To stop the enzyme reaction, DNSA (0.5 mL) is added to the mixture and kept in the boiling water bath for 90 min. After completion of the incubation time, diluted samples containing 0.5 mL are mixed with 2.5 mL of distilled water, and then it is measured by an Ultraviolet-Visible (UV-Vis) Spectrophotometer. Then the measured absorbance is compared with the control sample. Using the formula provided, the percentage inhibition of sample be calculated.

$$\%\ of\ inhibition = 100 * \left(\frac{Abs_c - Abs_{ext}}{Abs_c} \right) \quad \ldots (2)$$

where, Abs_{ext} is absorbance of test (plant extract + enzyme + substrate) and Abs_c is absorbance of control.

Analysis of anti-diabetic and anti-inflammatory activities using a bioactivity-aware machine learning framework

Given the small number of independently synthesized quinoline–carboxamide derivatives, the machine-learning framework optimized for controlling the complexity of the models and enhancing their generalization ability. Molecular descriptors and biological assay parameters obtained experimentally are used to develop a bioactivity prediction model. Compound-level validation used to prevent the over-optimistic estimation of the performance of the model due to the repeated concentration measurements of the same compound in both training and testing subsets. The developed framework validated by Leave-One-Compound-Out Cross Validation (LOCO-CV) in which all the synthesized compounds are completely excluded during model test. This approach offers a more accurate assessment of the model's ability to predict bioactivity of molecules that are not chemically observed. In addition, input features are carefully selected so as not to leak out information from the assay derived measurements. The proposed bioactivity prediction framework constructed with independent molecular and experimental descriptors such as molecular weight, structural descriptors and concentration levels. Biological assays-derived absorbance values are provided as experimental descriptors in addition to molecular and concentration-related to predict bioactivity. Absorbance data have been linked to percentage inhibition and so are interpreted carefully when used in the prediction process, and compound-level validation is used to reduce potential information leakage during model evaluation. Hence, the model only uses independent compound characteristics and experimental parameters that are known before the prediction of bioactivity. The architecture of the

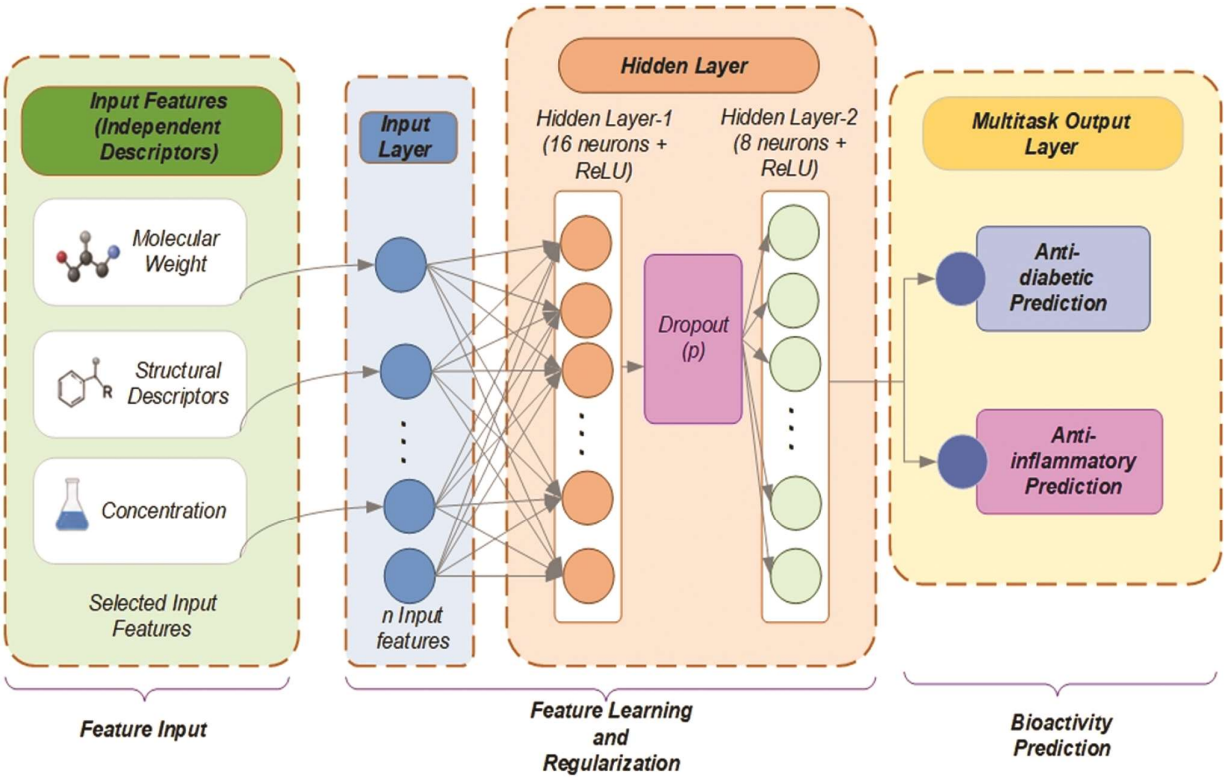


Fig. 3 — Architecture of the proposed compact neural network for multitask bioactivity prediction

proposed compact neural network for multitask bioactivity prediction has been depicted in (Fig. 3).

Compact Neural Network for Bioactivity Prediction

Considering the small number of compounds synthesized independently, a small neural network architecture used to limit the model complexity and the possible risk of overfitting. Independent molecular and experimental descriptors are selected as input to the model and it learns the nonlinear relationships related to anti-diabetic and anti-inflammatory activities. The input includes molecular weight, structure descriptors and concentrations. The values of absorbance for biological assays are used as experimental descriptors, yet the possible correlations between them and the calculated biological activity are carefully analyzed to reduce information leakage. The preprocessing and validation procedures are set up so that model evaluation is conducted based on compound-level data that is suitably separated from the target data to avoid direct transfer of target-related information during prediction.

The network is composed of two fully connected hidden layers of 16 and 8 neurons, respectively, and Rectified Linear Unit (ReLU) activation. Dropout is used during training to regularize the network and it helps to improve its generalization. The two biological activity endpoints are predicted by separate task-specific output nodes in a multitask learning framework. Leave-one-compound-out cross-validation is performed with the model, where all observations related to the test compound are completely hidden from the model development.

Multi-Task Learning for Dual Bioactivity Prediction

A multitask neural network is used to predict anti-diabetic and anti-inflammatory activities, with shared feature representations. The lower layer is trained to identify common relationships between molecular descriptors and bioactivity patterns, and the output layer is trained to make predictions specific to each of the biological endpoints. The model comprises several layers, which gradually convert raw input features, including the concentration of compounds, absorbance measurements, and molecular weight, into better representations, which increase the precision of predictions made about biological activity. The main elements of the DNN are the process of feature extraction, activation functions, and optimization methods. These aspects allow the model to learn successfully using various forms of data, including 1H- Nuclear Magnetic Resonance (NMR), Fourier

Table 3 — Specifications of the SMODNN Architecture

Parameter	Specification
Input features	Molecular weight, structural descriptors, concentration, and absorbance
Molecular features	Molecular weight and structural descriptors
Experimental features	Concentration and absorbance
Absorbance handling	Assay-derived experimental descriptor; evaluated separately because of its direct relationship with biological activity
Leakage-control strategy	Compound-level separation before preprocessing and model training; all measurements belonging to the held-out compound remain excluded from training
Validation strategy	Leave-One-Compound-Out Cross-Validation (LOCO-CV)
Test condition	One complete compound and all associated concentration/absorbance observations are held out in each fold
Network architecture	Compact neural network
Hidden layers	Dense (16, ReLU) → Dropout → Dense (8, ReLU)
Output	Anti-diabetic and anti-inflammatory bioactivity predictions
Interpretability	SHAP analysis, including the distribution of feature contributions

Transform Infrared (FT-IR), UV-visible spectroscopy, and biological assay outcomes such as BSA denaturation and alpha-amylase inhibition. Each of the hidden layers characterized by the following Equation (3) that allows learning the complex relationships between the structural descriptors and the biological activities they relate to in a more efficient way.

$$H_i = f\left(W_i H_{i-1} + B_i\right) \quad \ldots (3)$$

whereas, H_i denotes the i^{th} layer output, W_i states the weight matrix, B_i defines the bias term and f depicts the activation function (ReLU), and introduces non-linearity and an improvement in the model's capacity for understanding non-linear relationships between structural characteristics and biological activity. The activation function used by the ReLU is:

$$f(x) = \max(0, x) \quad \ldots (4)$$

Finally, for the output layer, a linear function is used to predict the bioactivity level and is given as

$$y = W_{out} . H_f + B_{out} \quad \ldots (5)$$

where y represents the predicted anti-diabetic or anti-inflammatory activity value, W_{out}. defines the weight matrix of the output layer, H_f states the final hidden layer output, B_{out} be the bias term of the output layer.

Enhancing Deep Neural Network Performance with Stochastic Multi-Objective Optimization (SMO)

Stochastic Multi-Objective Optimisation (SMO) improves DNN by balancing objective trade-offs, minimizing complexity, and optimizing hyperparameters. It optimizes model efficiency by ensuring that multiple conflicting objectives are handled simultaneously, such as reducing computational costs and improving prediction accuracy. The challenge of modeling biological activity involves handling large-scale, inconsistent data from biochemical assays and spectroscopic measurements, which are subject to variability and noise. These uncertainties are incorporated into the model through stochastic optimization, treating data parameters as random variables. Table 3 depicts the specifications of SMODNN Architecture.

The absorbance has been used as an experimental descriptor of the assay. To minimize train–test leakage across multiple measurements, compound-level separation is done prior to pre-processing and model training; all observations belonging to the held-out compound are hidden from the training set. Results containing absorbance are interpreted with caution as being bioactivity predictions based upon the assay conditions and not independent bioactivity predictions.

Let the objective function be $e(v, z)$ depend on the decision variable v and the random variable z, representing the input data. The expected objective function is:

$$E\left[\, e(v, z)\right] = \int e(v, z) p(z) dz \quad \ldots (6)$$

while, $p(z)$ defines the probability distribution of the stochastic biological activity data. This formulation accounts for uncertainties in experimental measurements and biological variability.

SMO improves the model by utilizing Sample Average Approximation (SAA):

$$Min\ e_m(v) = \frac{1}{m}\sum_{i=1}^{m} e(v, z_i) \quad \ldots (7)$$

whereas, m denotes the number of sampled data points, z_i be the i-th sampled realization of the random variable z.

The model parameters v are updated iteratively using stochastic gradient descent as:

$$v_{i+1} = v_i - \delta_i \nabla e(v_i, z_i) \quad \ldots (8)$$

where δ_i is the learning rate, and $\nabla e(v_i, z_i)$ represents the gradient of the objective function.

For multi-objective optimization addressing both anti-diabetic and anti-inflammatory predictions, the SMO formulation is extended as:

$$Min\ E(v) = \left(e_1(v), e_2(v)\right) \quad \ldots (9)$$

where, $e_1(v)$ and $e_2(v)$ represents the loss function for predicting anti-diabetic and anti-inflammatory activity. The framework employs multitask learning architecture where lower layers share representations between both bioactivity prediction tasks (anti-diabetic and anti-inflammatory). In contrast, task-specific branches in upper layers handle the unique characteristics of each activity type. This approach improves data efficiency and generalization performance. Figure 3 depicts the Proposed ResNet 50-based SMODNN framework.

Compound-Level Leave-One-Compound-Out Cross-Validation

With the small number of compounds synthesized independently from the quinoline–carboxamide class, the observations are not split and split–into–train separately, as this would allow measurements from the same compound to be included in both subsets. This partition could yield unrealistic predictive performance. Thus, leave one compound out cross validation (LOCO-CV) used to assess the compound level generalization.

The compounds are six independent ones (2a–2f), tested at several concentrations. One complete compound (and all observations corresponding to its concentration levels) excluded as the test set and the remaining six compounds are used to develop the model in each cross-validation fold. This repeated 6 times, each time using a different compound as an unseen test compound. Let the complete dataset be represented as:

$$D = \left\{D_{2a}, D_{2b}, ..., D_{2f}\right\} \quad \ldots (10)$$

where D_c contains all concentration-dependent observations for compound C. For fold k, the training and testing datasets are defined as follows:

$$D^{(k)}_{train} = \bigcup_{j \neq k} D,\ D^{(k)}_{test} = D_k \quad \ldots (11)$$

All the pre-processing parameters, such as feature scaling and model parameters, are optimized only on the training compounds of each fold. None of the held-out compound's measurements are involved in either training or preprocessing or hyperparameter selection. Therefore, the predictions generated are true out-of-compound predictions and not predictions on additional concentrations of compounds that are previously seen during the training.

Due to the limited number of independent chemical entities, a smaller ResNet-50 predictive architecture used instead of a larger version. The simplified architecture chosen to minimize the complexity of the model and the potential for overfitting. It is compared to traditional regression models using the same LOCO-CV protocol.

Results and Discussion

This section successfully synthesized a series of novel quinoline carboxamide derivatives (2a–2f) via amide coupling and comprehensively characterized them using multi-spectroscopic techniques (^{1}H NMR, ^{13}C NMR, FT-IR, UV-Vis, ESI-MS). The compounds are subsequently analysed for their *in vitro* anti-diabetic (α-amylase inhibition) and anti-inflammatory (BSA denaturation) activities. Furthermore, a ResNet-50-based Stochastic Multi-Objective Optimized Deep Neural Network (SMODNN) framework developed and benchmarked against conventional ML models to predict bioactivities from spectroscopic and physicochemical descriptors. The combined experimental and computational results provide strong evidence for the potential of these quinoline-carboxamide conjugates as dual-acting therapeutic candidates.

Analysis based on NMR spectrum

NMR is a highly adaptable spectroscopic process which is extensively employed in numerous research fields, specifically in chemistry. It is an essential method in contemporary science since it determines the chemical environments of atoms within

molecules. NMR has become integral to various areas of chemistry research, involving synthetic chemistry, catalysis, and chemical sensing [21-23]. NMR spectroscopy is commonly used for the analysis of synthesized intermediates and target compounds.

^{1}H- NMR spectral analysis

All the synthesized compounds contain a quinoline carbamide unit, which suggests that the compounds contain quinoline aromatic ring protons in their proton NMR spectra. There is a possibility that the carbamide -NH- peaks are present due to the highly exchangeable protons; otherwise, the peaks not be present in the NMR spectrum. Looking at the NMR spectrum, we notice that the aromatic protons from the quinoline present six aromatic protons in all the compounds.

From Figure 4, the carbamide NH proton peak is only seen in compounds 2a and 2c, showing a single proton counting after integration at approximately 10.5 ppm. Compound 2a also exhibited seven additional proton counts in the aromatic region, which correspond to the naphthalene unit. No other peaks are detected, indicating that the compound is pure [24-25]. Compound 2b had three additional peaks in the aromatic region, representing protons, as well as a singlet peak at 4.7 ppm, corresponding to two protons. The peaks correspond to the phenyl aromatic and methylene proton peaks. On the contrary, compound 2c exhibited only three proton counts other than the quinoline unit, which should correspond to di-chloro substituted phenyl ring. Compound 2d has only aliphatic substituents and showed three new peaks centered at 4.3 ppm, 4.2 ppm, and 1.3 ppm, which correspond to two methylene (-CH2-) and one methyl group (-CH3) from esters. The compound 2e revealed several peaks between 1.3 and 2.0 ppm, which accounted for ten hydrogen atoms. Later, it found to have a multiplet peak at approximately 4.0 ppm. The compound confirmed to have a cyclohexenyl ring. The NMR data for compound 2f showed nine peaks in the aliphatic region, which relates to the N-hexenyl ring. Further, three hydrogen counts are found, which merged with previous counts, corresponding to the S-Me group.

^{13}C- NMR spectral analysis

Figure 5 shows that the carbon NMR experiments are carried out on all the synthesized compounds. The analysis revealed the formation of the expected product. Notably, all the compounds in the carbon NMR spectrum exhibited the characteristic peaks of

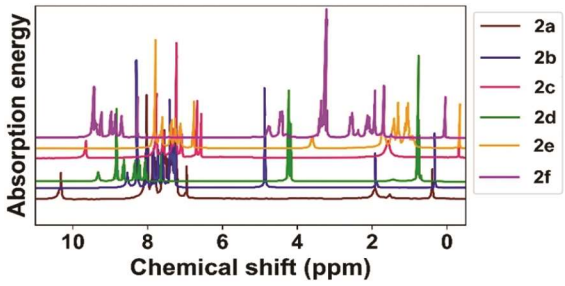


Fig. 4 — ^{1}H NMR spectrum for various compounds

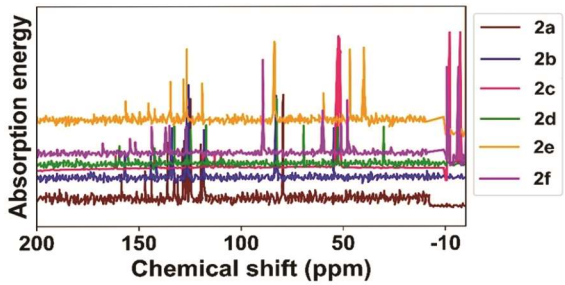


Fig. 5 — ^{13}C-NMR spectrum for various compounds

quinoline carboxamide carbon. Furthermore, it is worthy to note that the carbonyl carbon resonance of the carboxamide carbon appeared at ppm of 162, 164, 171, 164, 163, 163, accordingly, in compounds 2a-2f. In addition to that, in compound 2d, one more peak appears at 169 ppm; this peak is for the carbonyl carbon peak of the ester's functional group. Moreover, the peaks corresponding to all the carbons of the quinoline ring have shifted to respective aromatic region.

In addition to that, compound 2a-c has obtained extra peaks in the aromatic region, which is indicative of aromatic substitution carbons. Furthermore, the peak appears in compound 2b at 43 ppm, which is respectively for the methylene carbon peak. Similarly, in compound 2d, three peaks have appeared at ppm of 61, 43, and 14; these peaks are respectively for carbons of ester methylene, benzyl methylene, and ester methyl groups. For compound 2e, the four peaks that are obtained at ppm of 48, 33, 25, and 25, all of which are from the cyclohexyl ring. Lastly, compound 2f had four peaks that are obtained at ppm of 46, 45, 35, and 31, all of that are from the aliphatic ring and the S-methyl carbon functional group. The results that are obtained provided strong evidence regarding the proton NMR.

Analysis based on Fourier Transform Infrared (FT-IR) spectroscopy

Fourier Transform Infrared (FT-IR) spectroscopy serves as a crucial and dependable method for identifying functional groups within organic

molecules. Consequently, the synthesized compounds have been examined using FT-IR spectroscopy. Each of the synthesized compounds contains several functional groups such as quinolinyl, amide, aromatic, ester, methylene, chlorophenyl, and sulphonamide. As seen in Figure 6, the FT-IR spectra of the synthesized derivatives exhibit characteristic peaks for amide N–H[32], amide C=O[33], quinoline C=N[34], C–N[35], ester[36] and sulfonyl[37] functional groups, which is indicative of the presence of expected functional groups. Table 4 below demonstrates the stretching vibration of the existing functional groups within the synthesized compound. The absorption bands detected in the spectral range of 3348–3385 cm^{-1} are attributed to the N–H stretching vibrations of amide functions instead of C–H stretching vibrations of aromatic residues. The C–H stretching vibrations are generally seen in lower wavenumber regions while stretching vibration of hydrogen-bonded N–H are seen in higher wavenumber regions in the synthesized quinoline–carboxamide derivatives.

Furthermore, the quinoline C=N bond stretching is observed within the band of 1311-1385 cm^{-1}. The compound also contains the C-N stretching band of the existing quinoline within the band of 1285-1305 cm^{-1}. The amide carbonyl stretching

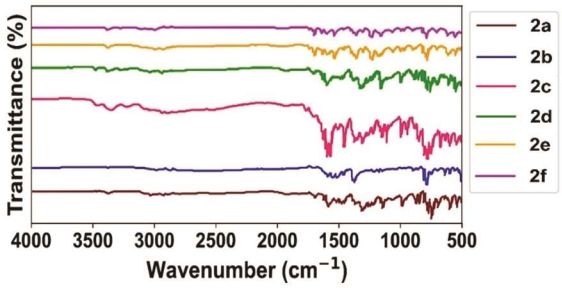


Fig. 6 — FT-IR spectra of all synthesized compounds at solid state

vibrations are observed in the region expected for the presence of the carboxamide linkage in the synthesized compounds. The differences in the carbonyl stretching frequencies of the various derivatives might be due to different electronic effects of the substituents and molecular environments. All the existing functional groups within the compound are confirmed through the obtained results. Furthermore, compound 2a has no functional group. However, compounds 2b and 2c have two different functional groups, such as methylene and chlorine substitution, showing peaks at 2980 cm^{-1} and 843 cm^{-1}, respectively. Moreover, the remaining three compounds have aliphatic chains, as their bond vibrations are detected in a range of 2935 cm^{-1} to 2989 cm^{-1}. Notably, compound 2d comprises an ester functional group, where its C=O and C-O bond-stretching frequency noted at 1688 cm^{-1} and 1145 cm^{-1}, correspondingly. Furthermore, compound 2f consists of a sulphonamide unit, which has resulted in S-C and S=O stretching frequencies at 1143 cm^{-1} and 1052 cm^{-1}, respectively. These results clearly confirm that the identification of compounds also justifies the NMR studies.

The assignments of the FT-IR are changed in view of the reported characteristic absorption ranges of amide, aromatic, ester and sulfonamide functional groups. The amide N–H stretching, amide carbonyl stretching, C–N stretching, quinoline C=N vibration, ester carbonyl vibration, and sulfonyl stretching bands are in favor of the successful synthesis of the proposed quinoline–carboxamide derivatives.

Analysis on Ultraviolet-visible (UV-Vis) and Electrospray Ionization Mass Spectrometry (ESI-MS)

The UV-Vis spectra of all synthesized compounds are recorded at room temperature in solution and are presented in (Fig. 7). Data shows two major bands are obtained for all the all-synthesized compounds. All the

Table 4 — FT-IR Spectral Assignments of Synthesized Quinoline–Carboxamide

Functional group	2a	2b	2c	2d	2e	2f
Amide N–H stretching	3406	3412	3468	3473	–	3474
Aromatic C–H stretching	–	2980	–	2935	2989	2984
Quinoline C=N stretching	1311	1385	1344	1311	1347	1372
Amide C=O stretching	1691	1594	1620	1621	1622	1684
Ester C=O stretching	–	–	–	1688	–	–
Ester C–O stretching	–	–	–	1145	–	–
Amide C–N stretching	1288	1285	1301	1294	1305	1286
C–Cl stretching	–	–	843	–	–	–
S–CH_3/S–C vibration	–	–	–	–	–	1143
S=O stretching	–	–	–	–	–	1052

compounds show a band around 236 nm, which might correspond to the quinoline ring carboxamide functional group. However, compound 2c doesn't show this band at the particular wavelength; hence, it's shifted to a higher wavelength (243 nm). The obtained band is not at a constant wavelength for all compounds. This observation is due to the presence of various kinds of substitutions lead to different wavelengths being obtained. For compounds 2a-2c, bands at higher regions are obtained at 284 nm, 286 nm, 294 nm, 261 nm, 289 nm, and 261 nm, respectively. Among these, compounds 2c and 2f have a great shift towards lower wavelength; also, compound 2c's band doesn't show rigid absorbance due to the presence of only aliphatic ethyl ester. This functional group is not influenced more in the spectra due to its lower absorbance ability. Moreover, compound 2f has superior absorbance with band shift, thus might be caused by the presence of the sulphonamide functional group, whereas other compounds have only a hydrocarbon functional group.

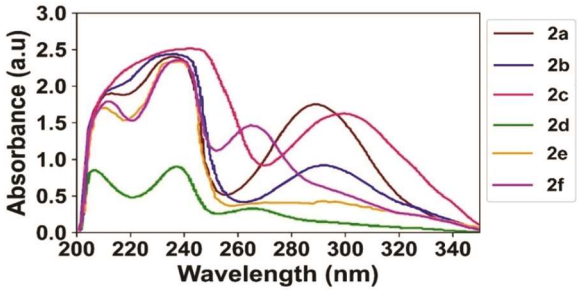


Fig. 7 — UV-Vis spectra of all synthesized compounds in methanol as a solvent

Further, synthesized compounds are structurally confirmed by ESI-MS spectroscopy given with supporting information in (Fig. 8). The obtained m/z values for all compounds are 299, 263, 316, 259, 255, and 332, respectively, for compounds 2a-2f. In this compounds 2a, 2d, and 2e have matched with M+1 ion peak, whereas compounds 2b and 2f have matched with M-1 ion peak, and also compound 2c is matched exactly with molecular ion peaks. The analytical characterization of synthesized compounds strongly suggested that compound's structure that given in (Scheme 1).

Biological Studies

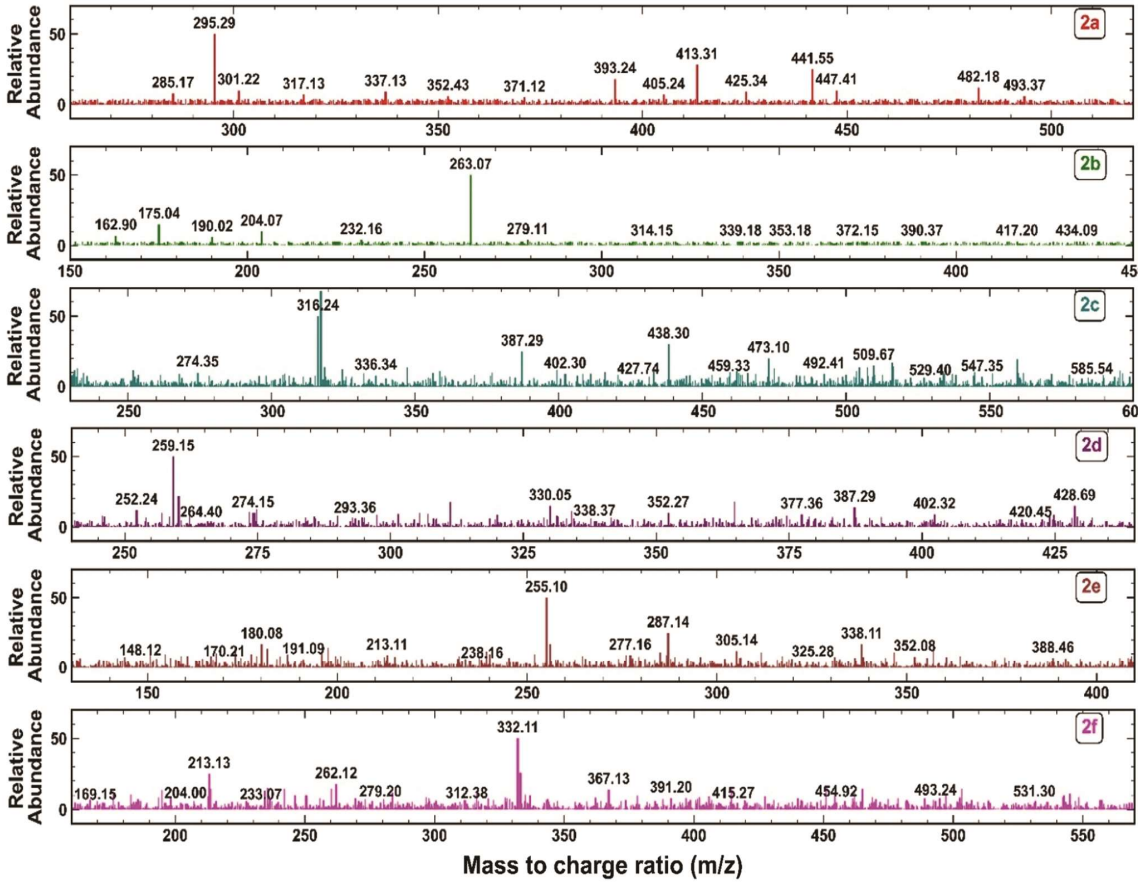
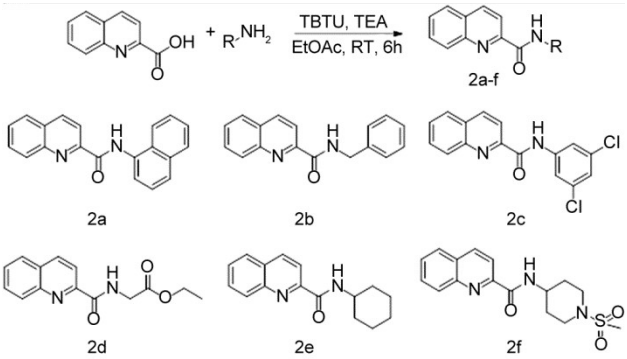


Fig. 8 — ESI-MS spectrum of various compounds (2a -2f)



Scheme 1 — Chemical synthesis of the quinoline compound and its derivatives

Each synthesized compound tested for its concentration-dependent inhibition, and the IC_{50} value calculated. Non-linear regression analysis of the percentage inhibition values obtained at various concentrations resulted in the construction of dose response curves. The concentration at which the activity inhibited by 50% used as the IC_{50} for the specific biological activity. The experimentally determined IC_{50} values are then converted to molar concentration units to calculate the corresponding $-\log_{10}(M)$ bioactivity values. The synthesized quinoline–carboxamide conjugates (2a–2f) are then analyzed for their *in vitro* anti-diabetic activity by α-amylase inhibition assay and anti-inflammatory activity by BSA protein denaturation assay. Triplicate experiments are performed for all biological experiments and the results are expressed as a mean value ± SD. All synthesized compounds and concentration levels are analyzed statistically in order to see the differences between them. Comparisons between multiple groups are done using a one-way analysis of variance (ANOVA) followed by Tukey's multiple comparison test. Statistically significant p-value considered < 0.05. Independent experimental measurements are used for statistical analysis instead of repeated technical measurements being used as distinct biological samples.

Anti-diabetic activity

Simple molecules are not like carbohydrates because they are composed of polymeric structures formed by sugar units that act as a source of energy during digestion. Various enzymes aid in breaking down these carbohydrates, resulting in the release of glucose molecules, which lead to spikes in blood sugar levels[26]. In the face of rising concerns over sugar consumption, scientists are opting to use other sugars such as allulose and sorbose to promote healthy lifestyle habits. However, the costs incurred during the production of such alternative sources pose a problem to their economic viability. Developing effective means to decrease or lower glucose compounds is believed to mark new avenues for the development of effective cures for diabetics. Of all the enzymes required during the metabolism of carbohydrates into sugar, α-amylase is seen to play a vital role. Thus, managing excessive α-amylase activity is thought to be a successful approach to treat diabetics.

The biological activity assessed at various concentrations of each of the synthesized compounds and the standard drug molecule so as to understand the concentration dependent activity. For a 400 mL concentration, most of the compounds showed a continued increase in the values of inhibition, comparable to the standard drug molecule. However, the activities of compound 2d and 2f are higher while comparing with the standard drug molecule. With the increase in concentration, most of the synthesized compounds showed activities comparable to or higher than the standard drug molecule, apart from 2e and 2b, whose activities reduced at high concentrations. The higher activity observed for compound 2f related to the presence of the sulfonamide containing substituent but this is a correlation for the synthesized compound series and needs further mechanistic studies to be confirmed. However, the compound intended to produce activity to the level of the standard drug molecule, implying that the role of both the functional group and the amide group is very significant. Table 5 illustrates the quantitative anti- diabetic activity of quinoline–carboxamide derivatives based on BSA protein denaturation assay.

Anti-inflammatory activity

Inflammation often serves as a precursor to various severe diseases, including cancer, which greatly reduce life expectancy[27-29]. Protein activity become irregular as a result, resulting in either heightened and diminished functionality. Excessive protein activity frequently leads to cell death. Therefore, the synthesized compounds are evaluated for inflammatory activity. In contrast to diabetic studies, all synthesized compounds demonstrated enhanced activity at lower concentrations, with the reference drug molecule exhibiting the least activity among them. The activity increase observed suggests that the synthesized compounds exhibited higher protein denaturation inhibitory activity than the control under

Table 5 — Quantitative Anti-diabetic Activity of Quinoline–Carboxamide Derivatives Based on α-Amylase Inhibition Assay

Compound	Concentration (µg/mL)	% Inhibition	Mean ± SD	IC_{50} (µg/mL)	95% CI	p-value
2a	100	42.6	42.6 ± 1.8	18.42	16.85–20.21	0.032
	200	56.8	56.8 ± 2.1			0.018
	300	68.4	68.4 ± 1.6			0.011
	400	78.2	78.2 ± 2.3			0.006
2b	100	39.8	39.8 ± 1.5	21.36	19.42–23.58	0.041
	200	53.7	53.7 ± 1.9			0.024
	300	65.9	65.9 ± 2.0			0.015
	400	74.6	74.6 ± 2.4			0.009
2c	100	45.2	45.2 ± 1.7	15.84	14.21–17.65	0.028
	200	60.5	60.5 ± 2.2			0.013
	300	72.6	72.6 ± 1.9			0.008
	400	82.1	82.1 ± 2.5			0.004
2d	100	48.5	48.5 ± 2.0	12.74	11.52–14.18	0.021
	200	65.4	65.4 ± 1.8			0.010
	300	77.8	77.8 ± 2.4			0.006
	400	86.5	86.5 ± 2.1			0.003
2e	100	44.1	44.1 ± 1.6	10.92	9.84–12.26	0.026
	200	63.8	63.8 ± 2.0			0.012
	300	79.4	79.4 ± 2.2			0.005
	400	88.3	88.3 ± 2.6			0.002
2f	100	52.4	52.4 ± 1.9	6.35	5.72–7.04	0.015
	200	70.8	70.8 ± 2.1			0.007
	300	84.7	84.7 ± 2.3			0.003
	400	91.6	91.6 ± 2.0			<0.001

the studied experimental conditions. The activity observed could be due to the presence of quinoline and amide functional groups; however, the molecular mechanism involved in the observed activity needs to be explored with target-specific biological assays. In addition, these derivative molecules that are incorporated onto each of these compounds are found to have no major influence on inhibition, thereby only varying these results by a slight degree. Notably, compound 2c demonstrated superior activities as its inhibition constant superior by seven points, while the other six compounds achieved superior results in higher points, ranging from 2 to 6, compared to the standard drug molecules.

The experimentally obtained IC_{50} values are converted from mass concentration units (µg/mL) to molar concentration units (M) using the molecular weight of each compound. Potency values are calculated for the corresponding using the following relationship:

$$-\log_{10}(M) = -\log_{10}\left(\frac{IC_{50}(\mu g/mL)\times 10^{-3}}{MW(g/mol)}\right) \quad \ldots (12)$$

where MW represents the molecular weight of the respective compound. Table 6 illustrates the quantitative anti-inflammatory activity of quinoline–carboxamide derivatives based on BSA protein denaturation assay.

Each biological parameter measured three times and mean ± SD calculated. Concentration-dependent inhibition curves are used to determine IC_{50} values by nonlinear regression analysis. The 95% confidence interval for the IC_{50} calculated from the fitted dose–response model to estimate the uncertainty in the estimation of the IC_{50}.

Analysis based on true bioactivity (-$\log_{10}$M) *vs* Concentration

The activity of synthesized quinoline–carboxamide derivatives (2a–2f) are expressed as $-\log_{10}(M)$ values, which are determined from their experimentally obtained IC_{50} values. The lower the $-\log_{10}(M)$ the more potent, as the less molar concentration that is required to achieve 50% inhibition. The values of $-\log_{10}(M)$ calculated are based on the experimentally determined IC_{50} values from (Tables 4 and 5), thus the potency comparison not just made from the graphical trends. The calculated $-\log_{10}(M)$ bioactivity values are based on the experimentally determined IC_{50} values (not on individual concentration points). Both the IC_{50} values derived from dose–response curve fitting is converted from molar concentration to $-\log_{11}(M)$ for comparative potency analysis.

For dose–response modelling, the inhibition response fitted by a nonlinear four-parameter logistic (4PL) model:

Table 6 — Quantitative Anti-inflammatory Activity of Quinoline–Carboxamide Derivatives Based on BSA Protein Denaturation Assay

Compound	Concentration (μg/mL)	% Inhibition	Mean ± SD	IC_{50} (μg/mL)	95% CI	p-value
2a	100	38.7	38.7 ± 1.7	16.84	15.21–18.46	0.039
	200	51.9	51.9 ± 2.0			0.021
	300	64.8	64.8 ± 1.8			0.012
	400	76.5	76.5 ± 2.2			0.006
2b	100	42.5	42.5 ± 1.6	14.92	13.45–16.37	0.031
	200	57.6	57.6 ± 2.1			0.016
	300	70.4	70.4 ± 2.3			0.008
	400	82.1	82.1 ± 2.0			0.004
2c	100	55.8	55.8 ± 1.9	11.48	10.32–12.76	0.018
	200	68.7	68.7 ± 2.2			0.009
	300	81.2	81.2 ± 2.4			0.004
	400	90.1	90.1 ± 2.5			<0.001
2d	100	50.4	50.4 ± 1.8	9.86	8.72–11.14	0.022
	200	66.5	66.5 ± 2.0			0.010
	300	79.3	79.3 ± 2.1			0.005
	400	88.6	88.6 ± 2.3			0.002
2e	100	53.6	53.6 ± 2.0	8.42	7.31–9.56	0.019
	200	69.8	69.8 ± 2.2			0.008
	300	83.5	83.5 ± 2.4			0.003
	400	91.4	91.4 ± 2.1			<0.001
2f	100	58.2	58.2 ± 1.8	5.75	5.12–6.43	0.012
	200	74.6	74.6 ± 2.0			0.006
	300	86.8	86.8 ± 2.3			0.002
	400	94.2	94.2 ± 2.5			<0.001

$$Y = Bottom + \frac{Top - Bottom}{1 + 10\left(LogIC_{50} - X\right) \times HillSlope} \quad \ldots (13)$$

where Y represents the percentage inhibition response, X represents the logarithm of concentration, Top and $Bottom$ indicate the upper and lower response limits, respectively, and $HillSlope$ describes the steepness of dose–response curve. The concentration corresponding to 50% inhibition obtained from the fitted IC_{50} parameter.

For anti-diabetic activity

The anti-diabetic activity of the synthesized quinoline–carboxamide derivatives (2a–2f) is assessed using the calculated $-\log_{10}$(M) values based on the experimentally determined IC_{50} values. In the synthesized compounds, compound 2f displayed the highest activity with $-\log_{10}$(M) value of 4.72 (lowest IC_{50} value of 6.35 μg/mL). Compounds 2e and 2d are comparatively potent having $-\log_{10}$(M) values 4.37 and 4.31 respectively. The potency value for compound 2c found to be moderate, 4.30, while 2a and 2b had moderate potency values of 4.21 and 4.09, respectively. The observed anti-diabetic activity of compound 2f, calculated by the molar potency, has been found to be the highest among the evaluated quinoline–carboxamide series.

For Anti-inflammatory Activity

The anti-inflammatory activity of the synthesized compounds evaluated by comparing their calculated $-\log_{10}$(M) values obtained from IC_{50} conversion. The most potent compound 2f with $-\log_{10}$(M) value of 4.76 (IC_{50} = 5.75 μg/mL) which had the lowest IC_{50} value among all the evaluated derivatives. Compounds 2e and 2c exhibited relatively higher potency values of 4.48 and 4.44, followed by compounds 2d (4.42), 2a (4.25), and 2b (4.25). The differences in the values of $-\log_{10}$(M) observed mean that there are differences in the potencies of the synthesized derivatives. Based on the results obtained from the BSA protein denaturation test, compound 2f appeared to possess the highest anti-inflammatory activity in the experimental conditions analyzed. Table 7 presents the calculated $-\log_{10}$(M) values for both anti-diabetic and anti-inflammatory activities, enabling direct comparison of the relative potency of the synthesized quinoline–carboxamide derivatives (2a–2f).

Table 7 — Conversion of IC_{50} Values to $-\log_{10}(M)$

Compound	Activity	IC_{50} (µg/mL)	Molecular Weight (g/mol)	IC_{50} (M)	$-\log_{10}(M)$
2a	Anti-diabetic	18.42	299	6.16×10^{-5}	4.21
	Anti-inflammatory	16.84		5.63×10^{-5}	4.25
2b	Anti-diabetic	21.36	263	8.12×10^{-5}	4.09
	Anti-inflammatory	14.92		5.67×10^{-5}	4.25
2c	Anti-diabetic	15.84	316	5.01×10^{-5}	4.3
	Anti-inflammatory	11.48		3.63×10^{-5}	4.44
2d	Anti-diabetic	12.74	259	4.92×10^{-5}	4.31
	Anti-inflammatory	9.86		3.81×10^{-5}	4.42
2e	Anti-diabetic	10.92	255	4.28×10^{-5}	4.37
	Anti-inflammatory	8.42		3.30×10^{-5}	4.48
2f	Anti-diabetic	6.35	332	1.91×10^{-5}	4.72
	Anti-inflammatory	5.75		1.73×10^{-5}	4.76

Analysis based on scatter plot: Actual *vs* Predicted values

Leave-one-compound-out cross-validation conducted to test the ability of the proposed framework to predict unseen compounds. In contrast to traditional random splitting, in this validation approach, all concentration measurements of the compound tested are completely excluded from model development. The final performance derived from the predictions of all six validation folds, which gives an unbiased estimate of the performance of the model at the compound level.

The compact multitask neural network compared with the conventional machine-learning approaches with compound-level LOCO-CV as shown in (Figs. 9a-d). A fair comparison of the predictive capability made with the same input features and validation settings. The Proposed Model of SMODNN is seen to perform well, yielding a perfect fit with values for R^2 of 1.00, and very low values for RMSE equal to 0.01, MAE=0.011 and MSE equal to 0.000. Although values of error increase marginally when tested (R^2 = 0.89, RMSE = 0.24, MSE = 0.056, MAE=0.189), the model's performance is seen to be quite good. Then the existing RF model perform well with values of R^2 equal to 0.99; although the values of the error, as far as the testing of the model is concerned, are increased (R^2 = 0.87, RMSE = 0.25, MSE = 0.062, MAE=0.211). Linear Regression has almost the same performance as the RF algorithm, showing a perfect fit for the training data (R^2 = 1.00) and a good fit for the test data (R^2 = 0.87). However, the errors show slightly higher values for Linear Regression, *i.e.*, RMSE = 0.25, MSE = 0.062, and MAE = 0.211, while the performance of the AdaBoost algorithm is poor, showing a lower value for the test data (R^2 = 0.42). It also shows the highest values for errors, *i.e.*, RMSE = 0.43 and MSE = 0.187, indicating poor performance due to overfitting. Hence, it is noticed that the performance of the Proposed SMODNN is quite good in understanding the complex structure-activity relationships. These observations suggest its potential performance as a robust and reliable tool for modelling structure-activity relationships for quinoline derivatives, representing its efficiency for solving the problem while considering the development of potential drugs for controlling different disorders, particularly anti-diabetic and anti-inflammatory.

The compound-level LOCO-CV evaluation provided a more conservative estimation of model generalization compared with the previous observation-level split is given in (Table 8). The proposed compact neural network exhibited an R^2 value of 0.83, which is higher than conventional machine-learning methods, and had lower RMSE and MAE values. Random Forest also performed well with an R2 of 0.78, while Linear Regression and AdaBoost had slightly lower predictive powers. The decrease in performance over conventional random splitting is because each validation fold is predicting on a completely unseen compound, rather than other concentration measurements of compounds already collected during training. The results show that the proposed framework is able to capture meaningful relations among molecular descriptors and biological activity and also to minimize the risk of data leakage.

Experimental descriptors used in the assays and independent molecular and experimental features are analyzed as absorbance measurements for the prediction of bioactivity. Absorbance values are therefore correlated with biological assay measurements and interpreted with caution and

Table 8 — Comparative Performance of ML Models Using Compound-Level LOCO-CV Validation

Model	Validation Strategy	R^2	RMSE	MAE
RF	LOCO-CV	0.78	0.31	0.245
Linear Regression	LOCO-CV	0.74	0.34	0.268
AdaBoost	LOCO-CV	0.62	0.42	0.335
Compact neural network (Proposed)	LOCO-CV	0.83	0.27	0.212

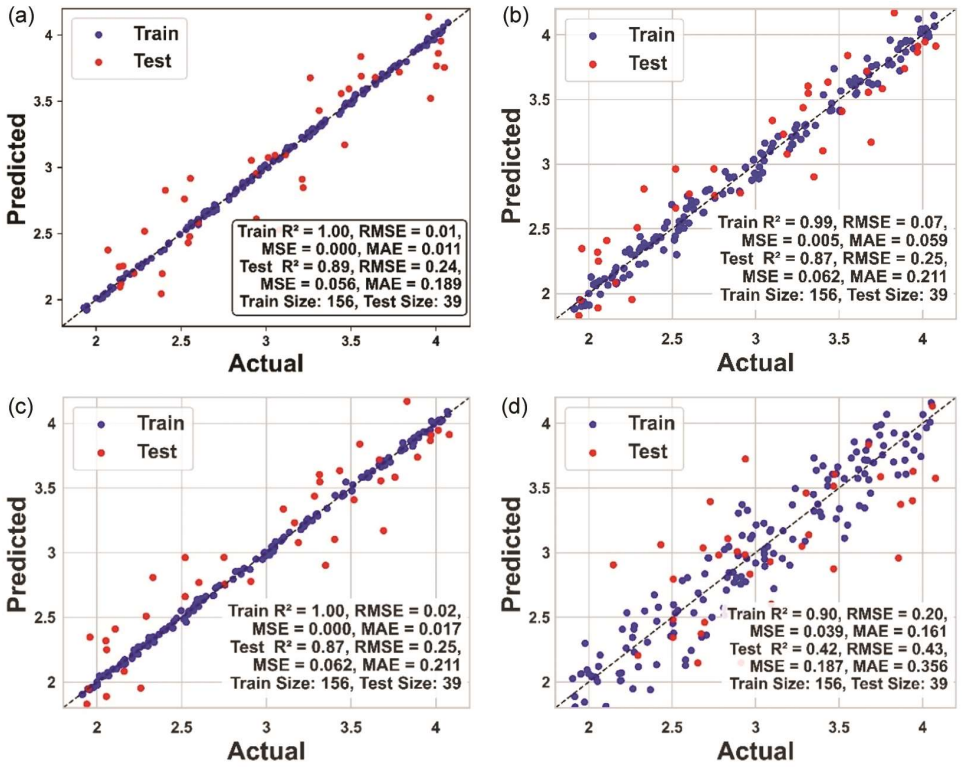


Fig. 9 — Analysis based on scatter plot: Actual *vs* Predicted Values

compound-level LOCO-CV used to mitigate potential information leakage due to overlapping compound-specific observations between training and testing datasets. The results obtained are bioactivity predictions that are informed by the assays, derived from the molecular and experimental descriptors.

SHAP analysis

To analyze the influence of the independent input features on the model predictions, the contribution to the model predictions investigated using the SHAP analysis. Analysis performed with the SHAP explainer that used the training samples as background/reference data set. As the dataset is relatively small and contains few independent compounds, the SHAP results are not generalizable to other datasets but rather interpreted as model insights specific to this dataset and should not be used to draw conclusions about biological significance. Based on

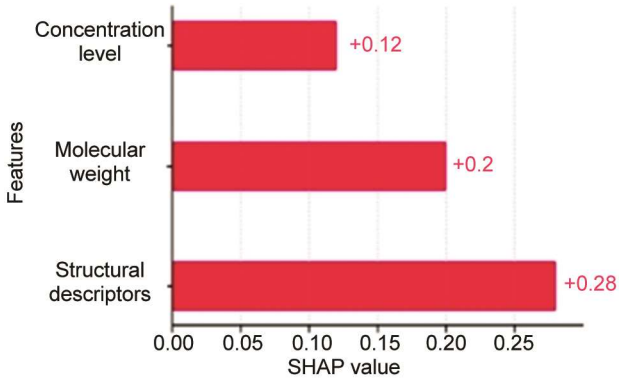


Fig. 10 — Distribution of SHAP values for independent features used in bioactivity prediction

Figure 10, it appears that the molecular weight the most significant of the input variables for the data set used in this research. Due to the limited number of independent compounds, however, the SHAP interpretation is regarded as an exploratory analysis in

Table 9 — Performance of the SHAP-Based SMODNN Model for Biological Activity Prediction

Method	Selected Inputs	Values	Target Parameter	Epochs and Structure of SMODNN	Training				Testing			
					R^2	RMSE	MSE	MAE	R^2	RMSE	MSE	MAE
SHAP	Molecular Weight	0.28	Anti-diabetic & Anti-inflammatory ($-\log_{10}M$)	150–200 epochs; 3-128-64-1 (ReLU, Dropout 0.5)	1.00	0.01	0	0.011	0.86	0.24	0.056	0.189
	Absorbance	0.20										
	Concentration	0.12										

the chemical series under investigation. In the same way, the updated set of independent variables used for SHAP analysis. The importance of molecular and experimental descriptors assessed in order to gain insight into how they affect the model predictions. Variations in hydrophobicity, aromatic substitution, and functional-group composition of the synthesized derivatives could play a role in the differences in biological response. These structural features, however, are only potential associations, based on the available data, and do not necessarily reflect specific biological mechanism. In addition, concentration corresponds to the lowest mean SHAP value of 0.12 among the three features, indicating a moderate impact on the model's prediction result. This ranking indicates that intrinsic molecular properties play a more dominant role in biological activity prediction than experimental concentration within the investigated range.

Molecular weight is the highest contributor of SHAP which means that the molecular weight descriptor had an impact on the model prediction in the data set investigated. Molecular weight alone should not be taken as an indicator of high biological activity, however. Rather, it could be due to a combination of molecular properties that include structural complexity, substituents and physicochemical properties, all of which contribute to the observed activity. The effect of the molecular descriptors could be due to variation in the physicochemical properties of the synthesized derivatives. However, these associations are only based on models and do not constitute evidence of enzyme interaction or specific biological mechanisms. The presence of an aromatic ring along with electron-withdrawing groups in 2c showed significant activity, thus supporting the importance of electronic transitions through indirect evidence of absorbance. This again supports the mechanistic consistency of the model prediction with the experimental results. Similarly, the concentration feature showed the lowest mean SHAP value, implying that despite the experimentally observed dose-dependent inhibition, the model's prediction is not influenced by the concentration. Instead, the intrinsic structural properties are the key drivers of the model's predictive output. This further supports the reliability of the model, confirming that it is not driven by trivial experimental conditions but rather by the underlying fundamental chemical properties.

In conclusion, the SHAP analysis considered an overall validation of the predictive framework. The consistency of the feature importance with the experimentally determined SAR trends confirms that the model is chemically meaningful and scientifically justified. The dominance of the Molecular Weight feature in the SHAP analysis and the experimentally determined SAR trends confirms the scientific credibility of the developed biological activity prediction system. Table 9 shows the performance of the SHAP-based SMODNN Model for Biological Activity Prediction.

External validation results

For validating its generalizability to other contexts, conducted an external validation with two the independent bioactive compounds from public databases. The selected data sets are not used for model training, optimization and internal validation. The dataset, "Bioactive compound isolation from Uromyrtus metrosideros and their structure characterization"[30] contains structurally characterized natural bioactive compounds, while another dataset, "The Parmodulin NRD-21 is an Allosteric Inhibitor of PAR1 Gq Signaling with Improved Anti-Inflammatory Activity and Stability"[31] contains compounds evaluated for anti-inflammatory activity.

For external evaluation, molecular descriptors of compounds are generated using the same descriptor extraction strategy applied to synthesized quinoline-carboxamide derivatives is shown in (Table 10). Trained ResNet-SMODNN model is directly used for these new compounds without any further training. Predicted bioactivity values are compared to

Table 10 — External Validation Performance

External Dataset	Prediction Task	R^2	RMSE	MAE
Bioactive compound isolation from Uromyrtus metrosideros and their structure characterization	Bioactivity prediction	0.76	0.38	0.29
The Parmodulin NRD-21 is an Allosteric Inhibitor of PAR1 Gq Signaling with Improved Anti-Inflammatory Activity and Stability	Anti-inflammatory activity prediction	0.81	0.32	0.25

experimentally measured activities for evaluating transferability and robustness over several chemical spaces.

Conclusion

This research presents the synthesis of a novel series of quinoline–carboxamide conjugates (2a–2f) and evaluates their anti-diabetic and anti-inflammatory activities through experimental and ML methods. Anti-diabetic activity achieved through α-amylase inhibition, while anti-inflammatory activity achieved through inhibition of BSA denaturation, in the synthesized compounds. Additional studies are needed to determine the molecular mechanisms underlying these biological effects in a target-specific manner. The proposed framework uses molecular and experimental descriptors such as molecular weight, structure, concentration level and absorbance values from assays to predict bioactivity. The contribution of absorbance is interpreted with caution as it is directly related to the calculation of biological activity; data separation at the compound level and LOCO-CV are used to minimize leakage between training and testing samples. The proposed SMODNN demonstrated superior predictive performance with a training R^2 of 1.00 and a test R^2 of 0.86, outperforming traditional ML techniques, including RF, Linear Regression, and AdaBoost in terms of lower MSE (0.056) and MAE (0.189) on the test set. Multitask learning was effectively integrated to simultaneously predict both anti-diabetic and anti-inflammatory activities, enhancing the generalization capability of the model. The results of the SHAP analysis showed that the molecular weight contributed most to the model's predictions in the current data set, giving interpretability to the model output. Therefore, the proposed framework is found to be suitable for the prediction of bioactivity of the investigated quinoline–carboxamide derivatives using ML approach. Leave-one-compound-out cross-validation gives a more conservative assessment of the predictive ability. Nevertheless, this research has been limited to a small number of synthesized compounds and a restricted range of chemical space. Future research will be done to validate this model with larger and more diverse chemical datasets involving independent external compound libraries for better generalization capability and wider applicability.

Conflict of interest

Both the authors declare no conflict of interest.

References

1 Avula SK, Ullah S, Halim SA, Khan A, Anwar MU, Csuk R & Al-Harrasi A, Synthesis of novel substituted quinoline derivatives as diabetics II inhibitors and along with their *in silico* studies. *J Mol Struct*, 1274 (2023) 134560.

2 Weyesa A & Mulugeta E, Recent advances in the synthesis of biologically and pharmaceutically active quinoline and its analogues: A review. *RSC Adv*, 10 (2020) 20784.

3 Govindarao K, Shirin D, Anjaleena D & Anusree P, Quinoline based 2-azetidinones, 4-thiazolidinones and their potential pharmacological activities. *J Pharma Insights Res*, 2 (2024) 107.

4 Macedo B, Ribeiro Vaz I & Taveira Gomes T, MedGAN: Optimized generative adversarial network with graph convolutional networks for novel molecule design. *Sci Rep*, 14 (2024).

5 Sun D, Wang B, Jiang Y, Kong Z, Mu M, Yang C, Tan J & Hu Y, Benzodioxane carboxamide derivatives as novel monoamine oxidase B inhibitors with antineuroinflammatory activity. *ACS Med Chem Lett*, 15 (2024) 798.

6 Itoh K, Kanzaki K, Ikebe T, Kuroita T, Tomozane H, Sonda S, Sato N, Haga K & Kawakita T, Synthesis and pharmacological evaluation of carboxamide derivatives as selective serotoninergic 5-HT4 receptor agonists. *Eur J Med Chem*, 34 (1999) 329.

7 Villarroel-Vicente C, García A, Zibar K, Schiel MA, Ferri J, Hennuyer N, Enriz RD, Staels B, Cortes D & Cabedo N, Synthesis of a new 2-prenylated quinoline as potential drug for metabolic syndrome with pan-PPAR activity and anti-inflammatory effects. *Bioorg Med Chem Lett*, 106 (2024) 129770.

8 Mukherjee S & Pal M, Medicinal chemistry of quinolines as emerging anti-inflammatory agents: An overview. *Curr Med Chem*, 20 (2013) 4386.

9 Hossain MS & Hussain MH, Multi-target drug design in Alzheimer's disease treatment: Emerging technologies, advantages, challenges, and limitations. *Pharmacol Res Perspect*, 13 (2025).

10 Bahal SM, Baichwal MR & Khorana ML, Studies on quinoline derivatives as anti-infective agents I. *J Pharm Sci*, 50 (1961) 127.

11 Şahin K, Sarıpınar E & Kılıçarslan S, Integrative 4D-QSAR and hybrid machine learning approaches for structure–activity relationship analysis of quinazolines derivatives. *SSRN*, (2025).

12 Sun J, Li ZH, Yang YF & Zhang SY, Machine learning for active sites prediction of quinoline derivatives. *Artif Intell Chem*, 3 (2025) 100082.

13 Naglah AM, Almehizia AA, Al-Wasidi AS, Alharbi AS, Alqarni MH, Hassan AS & Aboulthana WM, Exploring the potential biological activities of pyrazole-based Schiff bases as anti-diabetic, anti-Alzheimer's, anti-inflammatory, and cytotoxic agents: *In vitro* studies with computational predictions. *Pharmaceuticals*, 17 (2024) 655.

14 da Silva SE, da Silva Moura JA, Branco Júnior JF, de Moraes Gomes PA, de Paula SK, Francisco Viana DC, de Freitas Ramalho EA, de Melo Gomes JV, Pereira MC, da Rocha Pitta MG & da Rocha Pitta I, Synthesis and *in vitro* and *in silico* anti-inflammatory activity of new thiazolidinedione-quinoline derivatives. *Curr Top Med Chem*, 24 (2024) 1264.

15 Alharbi O, Alsaedi WH, Alsehli M, Althagafi SH, Alharbi HY, Asiri YM, Ramu R & Al-Ghorbani M, Novel quinoline- and naphthalene-incorporated hydrazineylidene–propenamide analogues as antidiabetic agents: Design, synthesis, and computational studies. *Pharmaceuticals*, 17 (2024) 1692.

16 Arabiyat S, Alzoubi A, Al-Daghistani H, Al-Hiari Y, Kasabri V & Alkhateeb R, Evaluation of quinoline-related carboxylic acid derivatives as prospective differentially antiproliferative, antioxidative, and anti-inflammatory agents. *Chem Biol Drug Des*, 104 (2024).

17 Aarjane M, Ghaleb A, Slassi S, Boubekri Y, Moussaoui O & Amine A, Synthesis, characterization and machine learning prediction of novel quinolone derivatives. *J Indian Chem Soc*, 102 (2025) 101976.

18 Marciniec K, Nowakowska J, Chrobak E, Bębenek E & Latocha M, Synthesis, docking, and machine learning studies of some novel quinolinesulfonamides–triazole hybrids with anticancer activity. *Molecules*, 29 (2024) 3158.

19 Nnyigide OS & Hyun K, The protection of bovine serum albumin against thermal denaturation and gelation by sodium dodecyl sulfate studied by rheology and molecular dynamics simulation. *Food Hydrocoll*, 103 (2020) 105656.

20 Sribalan R, Banuppriya G, Kirubavathi M, Jayachitra A & Padmini V, Multiple biological activities and molecular docking studies of newly synthesized 3-(pyridin-4-yl)-1H-pyrazole-5-carboxamide chalcone hybrids. *Bioorg Med Chem Lett*, 26 (2016) 5624.

21 Kotha S, Mehta G & Jena K, Synthetic approach toward diverse oxa-cages via olefin metathesis. *J Org Chem*, 89 (2024) 5952.

22 Arumugam SM, Mahala S, Devi B, Kumar S, Kunchala RK & Elumalai S, Molybdenum sulfide-2D nanosheets offering multiple metallic sites enable different sugar epimerization reactions to rare sugars in water. *React Chem Eng*, 8 (2023) 2641.

23 Senthil Murugan A, Kiruthika M, Abel Noelson ER, Yogapandi P & Annaraj J, Fluorescent sensor for *in vivo* bio-imaging, precise tracking of Fe3+ ions in zebrafish embryos and visual measuring of Cu2+ ions in picomolar level. *Arab J Chem*, 14 (2021) 102910.

24 Wang Z, The influence of AI on consumer behavior: Shaping choices and preferences in the digital marketplace. *Syst Soft Comput*, (2025).

25 Zhou F & Uddin S, FG-DDI: Functional group-aware graph neural networks for drug–drug interaction prediction. *J Biomed Inform*, 174 (2026) 104981.

26 Kaur N, Kumar V, Nayak SK, Wadhwa P, Kaur P & Sahu SK, Alpha-amylase as molecular target for treatment of diabetes mellitus: A comprehensive review. *Chem Biol Drug Des*, 98 (2021) 539.

27 Chen L, Deng H, Cui H, Fang J, Zuo Z, Deng J, Li Y, Wang X & Zhao L, Inflammatory responses and inflammation-associated diseases in organs. *Oncotarget*, 9 (2017) 7204.

28 Misiak B, Wójta-Kempa M, Samochowiec J, Schiweck C, Aichholzer M, Reif A, Samochowiec A & Stańczykiewicz B, Peripheral blood inflammatory markers in patients with attention deficit/hyperactivity disorder (ADHD): A systematic review and meta-analysis. *Prog Neuropsychopharmacol Biol Psychiatry*, 118 (2022) 110581.

29 Anand D, Colpo GD, Zeni G, Zeni CP & Teixeira AL, Attention-deficit/hyperactivity disorder and inflammation: What does current knowledge tell us? A systematic review. *Front Psychiatry*, 8 (2017) 228.

30 https://data.mendeley.com/datasets/ty35tfdhxc/2

31 https://data.mendeley.com/datasets/czfmhpjnpc/1

32 Kumar A, Kumar V, Nidhar M, Gill S & Tewari AK, Development of intermolecular amide-amide hydrogen-bonded synthon: Conformational stability and *in silico* studies. *Struct Chem*, (2026) 1.

33 Chai S, Zhang X, Li W, Xu M, Zhai S, Gong P, Zhang Y, Xia J, Li Y & Liu J, Amide methylation empowers concentrated hydrogel electrolytes for wide-temperature flexible aqueous sodium-ion batteries. *Energy Environ Mater*, (2026) e70514.

34 Kim YE, Kim J, Lee J & Hong S, Regiodivergent C3 and C4 amination of quinolines via radical and ionic pathways. *Angew Chem*, 138 (2026) e25818.

35 Khosravani P, Kebonye NM, Taghizadeh-Mehrjardi R, Shokati H, Hu L & Scholten T, Soil pH and latitude as a major predictor of C:N stoichiometry in Germany. *Catena*, 264 (2026) 109785.

36 Maarouf-Mesli N, Desjardins-Michaud J, Imani Z, Ghosh K, Polyak F & Lubell WD, Solvent-less environmentally benign amino ester, amide, and peptide synthesis enabled by resonant acoustic mixing. *Green Chem*, 28 (2026) 264.

37 Song XH, Meng SS, Wan YJ, Wang PF, Chan AS & Wang YJ, Sulfonyl-directed photoinduced dehydro-Diels–Alder reaction of aryl maleimides: Enabling regioselective naphthalene synthesis. *JACS Au*, 6 (2026) 534.